Preparation of a cattle bone collagen peptide-calcium chelate by the ultrasound method and its structural characterization, stability analysis, and bioactivity on MC3T3-E1 cells

Food and Function

Zhang, Hongru; Qi, Liwei; Wang, Xiaodan; Guo, Yujie; Liu, Jiqian et al

https://doi.org/10.1039/d2fo02146c

Food & Function

ROYAL SOCIETY OF CHEMISTRY

PAPER

View Article Online
View Journal | View Issue

Cite this: *Food Funct.*, 2023, **14**, 978

Preparation of a cattle bone collagen peptide–calcium chelate by the ultrasound method and its structural characterization, stability analysis, and bioactivity on MC3T3-E1 cells†

Hongru Zhang, [a,b] Liwei Qi,[a] Xiaodan Wang, [c] Yujie Guo,[a] Jiqian Liu,[a] Yang Xu,[e] Chengjiang Liu,*[d] Chunhui Zhang *[a] and Aurore Richel [b]

Received 23rd July 2022,
Accepted 5th December 2022

DOI: 10.1039/d2fo02146c

rsc.li/food-function

This study was designed to prepare a cattle bone-derived collagen peptide–calcium chelate by the ultrasound method (CP–Ca-US), and its structure, stability, and bioactivity on MC3T3-E1 cells were characterized. Single-factor experiments optimized the preparation conditions: ultrasound power 90 W, ultrasound time 40 min, $CaCl_2$/peptides ratio 1/2, pH 7. Under these conditions, the calcium-chelating ability reached 39.48 μg mg^{-1}. The result of Fourier transform-infrared spectroscopy indicated that carboxyl oxygen and amino nitrogen atoms were chelation sites. Morphological analysis indicated that CP–Ca-US was characterized by a porous surface and large particles. Stability analysis demonstrated that CP–Ca-US was stable in the thermal environment and under intestinal digestion. CP–Ca-US showed more stability in gastric juice than the chelate prepared by the hydrothermal method. Cell experiments indicated that CP–Ca-US increased osteoblast proliferation (proliferation rate 153% at a concentration of 300 μg mL^{-1}) and altered the cell cycle. Significantly, CP–Ca-US enhanced calcium absorption by interacting with calcium-sensing receptors and promoted the mineralization of MC3T3-E1 cells. This study provides the scientific basis for applying the ultrasound method to prepare peptide–calcium chelates and clarifies the positive role of chelates in bone building.

1. Introduction

Calcium is an essential micronutrient in bone building, intracellular metabolism, muscle contraction, blood coagulation, and oocyte activation. Calcium phosphate provides mechanical strength to teeth and bones, where 99% of the body's calcium exists. In 2001, the National Academy of Sciences of the United States indicated that adequate calcium intake is important for optimal peak bone mass and modulating aging-related bone loss.[1] Calcium deficiency is an increasing malnutrition, which could cause a variety of bone diseases including rickets and osteoporosis.[2,3] Calcium carbonate has been the most widely used calcium supplement for the past few decades. However, ionized calcium has disadvantages of biological toxicity at high concentrations and low bioavailability at low concentrations.[4]

Recently, peptide–calcium chelates have attracted widespread interest as a novel carrier to deliver calcium. Peptides could assemble with other molecules to form macromolecular structures *via* chemical bonds including coordination bonds, hydrophilic, hydrophobic, and electrostatic interactions, and ionic bonds.[5] Chelates can enhance the bioavailability of calcium due to their increased solubility and protective function against inhibitors in the digestive tract. Many peptides can resist the degradation in the gastrointestinal and plasma environment (such as pepsin, trypsin, and plasma protease) and reach integrally their target organs.[6,7] Therefore, peptide–calcium chelates could enhance calcium bioavailability and exert the bioactivity of peptides.[8] Many researchers are focusing on food protein-derived peptide–calcium chelates, such as

[a]*Key Laboratory of Agro-Products Processing, Ministry of Agriculture and Rural Affairs, Institute of Food Science and Technology, Chinese Academy of Agricultural Sciences, Beijing, 100193, China. E-mail: dr_zch@163.com*
[b]*Laboratory of Biomass and Green Technologies, University of Liege-Gembloux Agro-Bio Tech, Passage des Déportés 2, B-5030 Gembloux, Belgium*
[c]*Adaptation Physiology Group, Department of Animal Sciences, Wageningen University & Research, 6708 WD Wageningen, The Netherlands*
[d]*Institute of Agro-Products Processing Science, Technology Xinjiang Academy of Agricultural and Reclamation Science, Shihezi 832000, China. E-mail: lcj_5@sohu.com*
[e]*Inner Mongolia Peptide (Mengtai) Biological Engineering Co., Ltd, Shengle Economic Park, Helinger County, Hohhot, Inner Mongolia, 010000, China*
† Electronic supplementary information (ESI) available. See DOI: https://doi.org/10.1039/d2fo02146c

pig bone, chicken foot, milk, and tilapia bone.[9–12] Cattle is one of the most important livestock resources globally. In 2019, the global production of beef was about 62.9 million tons, and the yield of collagen-rich bovine bones, skins, and tendons was up to 31.4 million tons.[13] The protein content in cattle bone is 13.68–26.14 g per 100 g. More interestingly, collagen peptides derived from cattle bone have been evidenced to possess anti-osteoporosis function.[14] From economic, environmental protection, and human health perspectives, the high-value utilization of cattle bone resources is of great significance.

The preparation method of peptide–calcium chelates is usually the hydrothermal method. In solution, peptides could aggregate to form amorphous or highly structured amyloid-like fibrils, which may limit the chelating ability of peptides.[15] With the development of innovative food processing technologies, the ultrasound method, one of the innovative technologies, has been more widely considered.[16,17] The ultrasound method is an eco-friendly, effective, safe, and non-toxic technology (ultrasonic waves above 20 kHz). Ultrasound produces powerful forces at the microscopic scale by shock causing chemical changes in the medium.[18] Ultrasound could produce cavitation, which can change the protein structure and expose more groups, meaning more chelation sites between peptides and Ca^{2+}.[16] It was also demonstrated that ultrasound treatment can decrease the aggregation of peptides to a small and uniform structure. Ultrasound treatment has been widely applied to extract proteins and peptides from natural products, facilitating higher yields and extraction rates.[19] To the best of our knowledge, there are few reports about the application of the ultrasound method in peptide–calcium chelate preparation. The cavitation pressure and high temperature caused by ultrasonic treatment can accelerate the progress of chemical reactions, promote the mutual penetration of molecules and open chemical bonds. At the same time, it can further accelerate the chelation reaction through the absorption of sound, the secondary effects caused by the resonance properties of the medium and the container. Therefore, we predicted that the ultrasound method can be applied for preparing chelates. In particular, studies related to the effects of the hydrothermal method and ultrasound method on the structure of chelates are limited. Current research is mainly focused on the isolation of calcium-binding peptides, structural analysis, and transportation across Caco-2 cells.[10,11] Several studies demonstrated that peptide–calcium chelates could promote intestinal calcium absorption.[11,20] Therefore, based on previous studies, we investigated the bone formation bioactivity of chelates by cellular experiment of murine osteoblasts MC3T3-E1.

The primary purpose of the present study was to prepare a cattle bone collagen-derived peptide–calcium chelate by the ultrasound method. Single-factor experiments optimized the processing conditions. The amino acid composition, Fourier transform-infrared spectroscopy (FT-IR), molecular mass distribution, thermogravimetric analysis (TGA), stability of CP–Ca-US, and its biological function on MC3T3-E1 cells were determined.

2. Materials and methods

2.1. Materials

Cattle bone-derived collagen peptides were provided by Inner Mongolia Peptide (Mengtai) Biological Engineering Co., Ltd (Inner Mongolia province, China). The collagen peptides were isolated by hot-pressure and enzymatic hydrolysis from cattle bone. The protein purity reached was 93.2%. The molecular weight was mainly <500 Da (78.7%). The amino acid composition of collagen peptides is shown in Fig. 2E in detail. Calcium chloride was purchased from Sigma-Aldrich (St Louis, MO, USA). Murine osteoblast MC3T3-E1 cells, α-MEM medium, fetal bovine serum, and osteogenic differentiation medium were purchased from Procell Life Science & Technology Co., Ltd.

2.2. Preparation experiment of peptide–calcium chelate by the ultrasound method

Collagen peptides were dissolved in ultrapure water (50 mg mL^{-1}), and then $CaCl_2$ was added. The above solution was mixed thoroughly by a vortex mixer for 1 min in a 30 mL glass bottle. Then, CP–Ca-US was prepared by ultrasound (20–25 kHz) using an ultrasonic cell disruptor (Scientz-IID, Ningbo Xinzhi Biotechnology Co., Ltd, Ningbo, China). According to previous pre-experiments and literature review, the optimized process parameters included ultrasound power (60–180 W), ultrasound time (20–60 min), $CaCl_2$/peptides ratio (1/6–1/2), and pH value (5–9). To exclude the influence of temperature on the chelation process, the glass bottle was placed in an ice-water bath, and the temperature was controlled within a stable range (4.46 ± 0.26 °C) detected by a temperature recorder (L93-1, Hangzhou Loggertech Co., Ltd, Hangzhou, China). After the chelation reaction, 9 times volume ethanol was added to the chelated solution to precipitate the collagen peptide–calcium chelate and the chelate and calcium ions were separated. Then, the precipitate was washed with 90% ethanol several times to remove free calcium ions as far as possible. Finally, the above solution was centrifuged at 8000*g* for 15 min. The obtained precipitate was lyophilized and marked as CP–Ca-US. The schematic diagram is shown in Fig. 1A.

The chelate prepared by the hydrothermal method according to a previous study was used as a control.[21] Collagen peptides were dissolved in ultrapure water, and then $CaCl_2$ was added ($CaCl_2$/peptides, w/w, 1/5). The solution was stirred at 60 °C for 60 min to obtain the peptide–calcium chelate. After the chelation reaction, 9 times volume ethanol was added to the chelated solution to precipitate the collagen peptide–calcium chelate and the chelate and calcium ions were separated. Then, the precipitate was washed with 90% ethanol several times to remove free calcium ions as far as possible. Finally, the above solution was centrifuged at 8000*g* for 15 min. The precipitate was collected after lyophilizing and recorded as CP–Ca-HT. The calcium content of CP–Ca-HT and CP–Ca-US was detected to describe the calcium-chelating ability (CCA). The yield was computed from chelate = recycled chelate (g)/added collagen peptides (g).

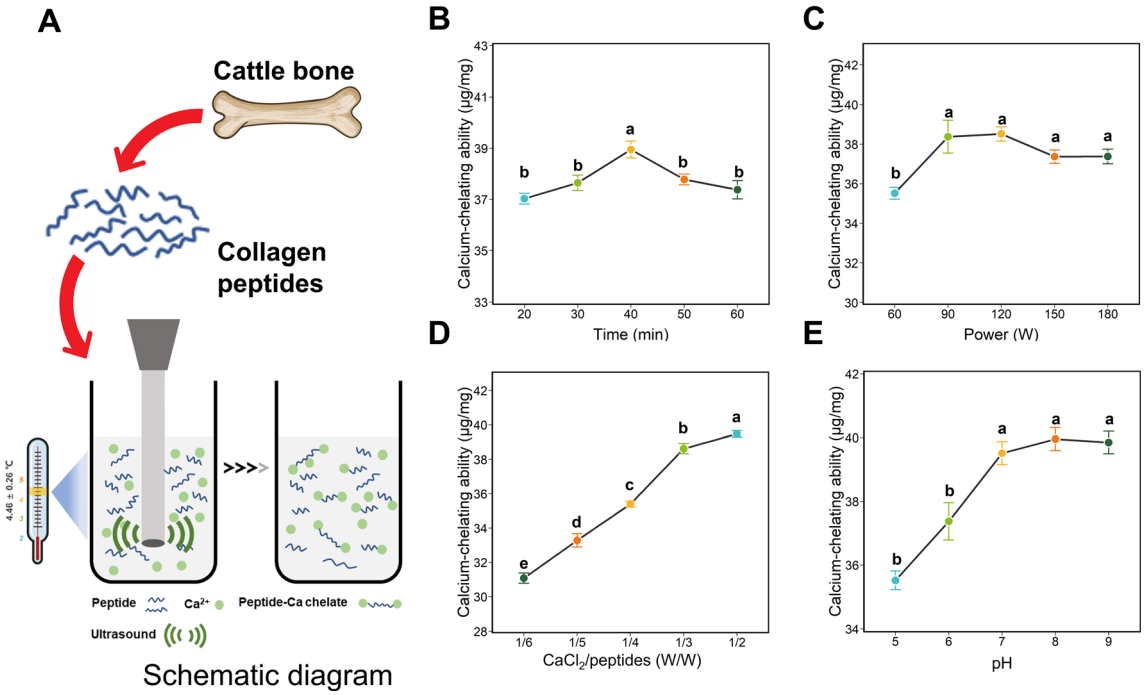

Fig. 1 (A) Schematic representation of fabricating CP–Ca-US by the ultrasound method, calcium-chelating ability affected by (B) ultrasound time, (C) ultrasound power, (D) $CaCl_2$/peptides ratio, and (E) pH value. Duncan's test was used to evaluate the significant differences between different groups. The different letters mean a significant difference between the two groups.

2.3. Molecular weight determination

The molecular weight of the samples was determined by a HPLC apparatus (Agilent 1260) equipped with DAWN HELEOS-II (Wyatt Technology Corporation, America) and Optilabr EX (Wyatt Technology Corporation, USA) detectors, and a TSK gel G4000PWxl column (7.8 × 300 mm, TOSOH, Tokyo, Japan). Briefly, the mobile phase consisted of 54.9% ultrapure water, 0.1% trifluoroacetic acid, and 45% acetonitrile. The standard sample was composed of Gly–Sar (146 Da), Gly–Gly–Tyr–Arg (451 Da), bacitracin (1422 Da), aprotinin (6511 Da), and cytochrome C (12 327 Da), purchased from Sigma-Aldrich (St Louis, MO, USA).

2.4. Amino acid analysis

The amino acid contents of CP, CP–Ca-HT, and CP–Ca-US samples were determined by an amino acid automatic analyzer (L-8900, Hitachi Ltd, Japan). The sample was hydrolyzed with 6 M HCl at 110 °C for 24 h. Before amino acid analysis, the hydrolysate was filtered using filter membrane to remove impurities.

2.5. Fourier transform-infrared (FT-IR) spectroscopy

The FT-IR spectra of the CP, CP–Ca-HT, and CP–Ca-US samples were analyzed with an FT-IR spectrometer (Tensor-27, Bruker Company, Germany). The mixture of the dried sample powder and KBr powder was thoroughly ground and compressed into a tablet, and KBr powder was applied as the background. The FT-IR spectra were obtained in the wavenumbers ranging from 4000 to 400 cm^{-1} and the spectral resolution was 4 cm^{-1}.

2.6. Circular dichroism (CD) spectroscopy

The secondary structure of the CP, CP–Ca-HT, and CP–Ca-US samples was determined by circular dichroism spectroscopy (Jasco Co., Jasco J-810, Tokyo, Japan) according to a previous study.[22] Each sample was solubilized in ultrapure water at 1 mg mL^{-1} concentration before detection. CD spectra were determined at 190–260 nm with a 2 nm slit. The percentage composition of the secondary structure was determined by the Spectra Manager Version 2.1.1.1 software (JASCO Co., Tokyo, Japan).

2.7. Scanning electron microscopy (SEM)

Scanning electron microscopy images were obtained to present the microstructure of CP, CP–Ca-HT, and CP–Ca-US by a scanning electron microscope (Zeiss Merlin Compact, Germany) equipped with energy dispersive spectroscopy (EDS) under a 10 kV accelerating voltage. Before obtaining SEM and elemental mapping images, the sample was sprayed with gold plating film.

2.8. Atomic force microscopy (AFM)

Atomic force microscopy images were obtained by atomic force microscopy (AFM, NX-10, Park Systems). The sample solution (20 μL, 10 mg mL^{-1} sample) was dropped on mica sheet. The scanning image was observed under the tapping mode at 15 kV.

2.9. Thermal gravimetric analysis (TGA)

The thermal property of CP, CP–Ca-HT, and CP–Ca-US was determined by a thermal gravimetric analyzer (Pyris Diamond TG/DTA, PerkinElmer, USA) from 30 to 500 °C at 10 °C min^{-1} under a N_2 atmosphere.

2.10. Stability analysis

The stability analysis was conducted according to a previous study.[21] An aqueous solution of CP–Ca-US (10 mg mL^{-1}) was heated to different temperatures (50, 60, 70, 80 °C) and incubated for 1 h (pH 7). After incubation, the heated solution was mixed with ethanol and then centrifuged at 8000*g* for 15 min to obtain the chelate. The stability of CP–Ca-US against gastrointestinal digestion *in vitro* was determined. CP–Ca-US dissolved in ultrapure water with gastric pH (2.0) and intestinal pH (7.5), respectively. Next, CP–Ca-US was dissolved in simulated human gastric juice (A7920, Solarbio, Beijing, China) and simulated human intestinal juice (A1790, Solarbio, Beijing, China). The above solution was incubated at 37 °C for 1 h. To terminate digestion, the solution was heated at 100 °C for 10 min. The chelate of CP–Ca-US in the control group was serially dissolved in distilled water at 22 °C for 1 h, and the solution was mixed with ethanol and then centrifuged at 8000*g* for 15 min to obtain the chelate. The calcium content in the chelate was analyzed using an atomic absorption spectrophotometer. The formula for the calcium retention rate was as follows:

$$\text{Calcium retention rate}\,(\%) = \frac{\text{Calcium content in treatment group}}{\text{Calcium content in control group}} \times 100$$

2.11. Cell proliferation

MC3T3-E1 cells were cultured in α-MEM medium supplemented with 10% fetal bovine serum. The cells were cultured in a cell incubator at 37 °C and 5% CO_2. The cells were seeded at 5000 cells per well in a 96-well plate. After 24 h of incubation, MC3T3-E1 cells were treated with $CaCl_2$ (9.24 μg mL^{-1}), mixture of CP (71.67 μg mL^{-1}) and $CaCl_2$ (9.24 μg mL^{-1}), CP–Ca-HT (75 μg mL^{-1}), and CP–Ca-US (75 μg mL^{-1}, 100 μg mL^{-1}, 200 μg mL^{-1}, 300 μg mL^{-1}) for 72 h. In the mixture of CP and $CaCl_2$, peptide and calcium content was equal to that in CP–Ca-US (75 μg mL^{-1}). The calcium content in CP–Ca-US was similar to that in CP–Ca-HT. Cells treated with the medium (without sample) were used as the normal group. An MTT cell assay (C0009S, Beyotime) kit was applied to detect cell proliferation according to the manufacturer's instructions.

2.12. Cell cycle assay

After culturing of the MC3T3-E1 cells exposed to the medium with $CaCl_2$ (9.24 μg mL^{-1}), mixture of CP (71.67 μg mL^{-1}) and $CaCl_2$ (9.24 μg mL^{-1}), CP–Ca-HT (75 μg mL^{-1}), and CP–Ca-US (75 μg mL^{-1}, 150 μg mL^{-1}, 300 μg mL^{-1}) for 72 h and normal medium for 72 h, the cell cycle was analyzed by DNA content quantitation assay (CA1510-20T, Solarbio, Beijing, China) with a flow cytometer (CytoFLEX, Beckman Coulter, Germany).

2.13. Confocal laser scanning microscopy (CLSM)

Intracellular calcium ions of MC3T3-E1 cells were determined by CLSM (LSM880, ZEISS, Germany). MC3T3-E1 cells were cultured with $CaCl_2$ (36.63 μg mL^{-1}), mixture of CP (286.68 μg mL^{-1}) and $CaCl_2$ (36.63 μg mL^{-1}), CP–Ca-HT (300 μg mL^{-1}), CP–Ca-US (300 μg mL^{-1}), CP–Ca-US (300 μg mL^{-1}) + R568 (CaSR agonist, 5 μM), and CP–Ca-US (300 μg mL^{-1}) + Calhex231 (CaSR inhibitor, 3 μM) for 24 h. In the mixture of CP and $CaCl_2$, peptide and calcium content was equal to that in the chelate. After cultivation, MC3T3-E1 cells were washed with phosphate buffer solution (PBS) and were stained with 5 μM Fluo-4/AM (S1060, Beyotime Biotechnology) for 30 min at 37 °C in the dark. Then, 2 μg of Hoechst 33342 (C1029, Beyotime Biotechnology) was added to stain the living cells being cultured at 37 °C for 5 min in the dark. The fluorescence of calcium ions was measured by CLSM. ImageJ software was used to quantify fluorescence intensity.

2.14. Mineralization assay

MC3T3-E1 cells were seeded in a 12-well plate and cultured by osteogenic differentiation medium with $CaCl_2$ (9.24 μg mL^{-1}), mixture of CP (71.67 μg mL^{-1}) and $CaCl_2$ (9.24 μg mL^{-1}), CP–Ca-HT (75 μg mL^{-1}), and CP–Ca-US (75 μg mL^{-1}, 100 μg mL^{-1}, 200 μg mL^{-1}, 300 μg mL^{-1}). The cells of the normal group were cultured by osteogenic differentiation medium. In the mixture of CP and $CaCl_2$, peptide and calcium content was equal to that in the chelate. The calcium content in CP–Ca-US was similar to that in CP–Ca-HT. After 21 days of cultivation, the cells were washed twice with PBS. Alizarin Red S (pH 4.2, Beyotime) was used to stain cells for 30 min at 22 ± 4 °C. Then, to remove the unbound dye, cells were washed with distilled water. The mineralization image was observed using an inverted microscope (IX51, Olympus, Japan). To quantify the bound dye, the cells were destained with 10% cetylpyridinium chloride in the dark for 1 h. The concentration of the solubilized Alizarin Red S was measured at 570 nm.

2.15. Molecular docking

The three-dimensional structure of calcium/calmodulin mediated calcium/calmodulin-dependent protein kinase (CaMKII) was obtained from the RCSB Protein Data Bank (PDB ID: 5IG1). Before docking, the structure of CaMKII was prepared by removing water and ligands, adding polar hydrogen. For peptides, the CHARMm forcefield was simulated and subsequently minimized using the Smart Minimizer method, with 2000 maximum steps and an RMS gradient of 0.01. After these pretreatments, the CDOCKER procedure of Discovery Studio 2019 (BIOVIA) was used to carry out molecular docking. Only one conformation with the lowest docking energy was retained. CaMKII and peptides were defined as the receptor and as ligands, respectively.

2.16. Statistical analyses

R project 4.0 (R Core Team) was used to analyse the data. Analysis of Variance (ANOVA) along with Duncan's multiple com-

parisons was performed on the obtained data (calcium-chelating ability, secondary structure, cell proliferation, cell cycle, and intracellular calcium ions). One-way ANOVA was performed on the amino acid content and calcium retention rate data. *P*-Value < 0.05 was considered statistically significant. All data were expressed as the mean ± SD (standard deviation). The ggplot2 package of R project was used for data visualization.

3. Results and discussion

3.1. Effect of process conditions on calcium-chelating ability

To optimize the preparation process of the peptide–calcium chelate by the ultrasound method, the effects of ultrasound power (W), ultrasound time (min), $CaCl_2$/peptides (weight/weight, w/w) ratio, and pH value on CCA were evaluated. Except for the experimental variable, the process conditions were selected as follows: pH 7, ultrasound power 120 W, ultrasound time 30 min, $CaCl_2$/peptides ratio 1/2. Ultrasound time and ultrasound power were regarded as the main factors affecting the chemical reaction. Meanwhile, our previous study demonstrated that the $CaCl_2$/peptides ratio and pH value also obviously influenced the CCA.[21]

In Fig. 1B, as ultrasound time increased from 20 to 40 min, the CCA reached a peak value of 38.95 μg g^{-1}. However, when ultrasound time was extended to 60 min, the CCA showed a downward trend. The increased ultrasound temperature can accelerate the interaction of peptide molecules and calcium ions to form a chelate. However, excessive ultrasound may cause coordination bonds to break due to the continuous increase of hydrogen ion concentration in water.[24] When the ultrasound time exceeded 40 min, the aggregation of collagen peptides played a major role, thereby reducing the solubility of peptides and the ability of peptides to bind calcium. Gülseren *et al.*[25] indicated that the particle size of bovine serum albumin increased up to 3.4 times after 90 min of ultrasound treatment. In Fig. 1C, as ultrasound power varied from 60 W to 120 W, the CCA reached a maximum value of 38.52 μg g^{-1} at 120 W. There was no significant difference between 90 and 180 W. The CCA increased rapidly under low ultrasound power (60–120 W), then showed a decreasing trend under high ultrasound power (120–180 W). Under low ultrasound power, since ultrasound cavitation destroyed noncovalent bonds (hydrophobic interaction, electrostatic interaction and hydrogen bonding), large peptide clusters became smaller fragments. As the ultrasound power was increased up to a certain point, the effect of ultrasound on the chelation reaction reached a balance. When the power was too large, it would destroy the coordination bond between peptides and calcium ions. The ultrasound treatment promoted changes in the secondary structure of collagen peptides producing an intermediary molten globule state, in which denaturation and aggregation occurred.[26] The excess radicals caused by the ultrasound cavitation effect might enhance the movement of protein molecules and increase the chance of collisions between protein molecules, leading to an increase of the particle size. The large sized particles were not conducive to the chelation reaction between collagen peptides and calcium ions. Thus, with the increase of ultrasonic power (>120 W) and ultrasonic time (>40 min), the content of insoluble peptides increased, so that the CCA decreased. As shown in Fig. 1D, with the increase in the $CaCl_2$/peptides ratio from 1/6 to 1/2, the CCA significantly increased. The increased calcium ion ratio meant more contact opportunities between the peptide molecules and calcium ions. As shown in Fig. 1E, with increasing pH from 5 to 10, the CCA increased significantly (pH 5–7) and then no significant change (pH 7–9) was seen. In the neutral or alkaline environment, the hydrogen ion concentration decreased, which could improve the coordination between Ca^{2+} with NH^{3+} and $COOH^{-}$.

The optimized preparation conditions of the ultrasound method were as follows: ultrasound time 40 min, ultrasound power 90 W, $CaCl_2$/peptides ratio 1/2, and pH 7, according to the above results. Under these process parameters, the CCA reached 39.48 ± 0.19 μg mg^{-1}. Meanwhile, no significant difference was observed between the hydrothermal method (44 ± 4%) and ultrasound method (41 ± 6%) in the yield of chelate. Previous studies demonstrated similar results: the CCA of sea cucumber ovum hydrolysate reached 53.45 mg g^{-1}, and the CCA of egg white peptides reached 44 mg g^{-1}.[27,28] Liao *et al.*[9] isolated three peptides from tilapia bone collagen hydrolysate, and the CCA of peptides reached 18.80, 35.73, and 28.4 mg g^{-1}, respectively. The CCA of this study was similar to the above-mentioned studies and lower than some studies. The main reason may be that the low-temperature environment (4.46 ± 0.26 °C) in this study was not conducive to the formation of a peptide–calcium chelate. The ultrasound process is often accompanied by an increase of temperature, which could promote the chelation reaction. The CCA will show a higher value if cooling is not performed in the ultrasound method.

3.2. Structural characterization

3.2.1. FT-IR analysis. The characteristic change of FT-IR spectra is used to determine interactions between metal ions and organic groups. As shown in Fig. 2A, after the chelation reaction, the band of CP (3273.95 cm^{-1}) shifted to 3385.28 cm (CP–Ca-HT) and 3400.74 cm^{-1} (CP–Ca-US), which may be due to the combination between $–NH_2$ and Ca^{2+}.[29] The stretching of NH enabled N–Ca to replace hydrogen bonds. The FT-IR spectra indicated that the wavenumber at 1656.00 cm^{-1} (CP) of the amide I band shifted to 1657.27 cm^{-1} (CP–Ca-HT) and 1657.36 cm^{-1} (CP–Ca-US) after peptides bound to calcium, which is due to the C═O stretching vibrations. The band at 1401.49 cm^{-1} for the –COO– groups in CP moved to 1407.44 cm^{-1} (CP–Ca-HT) and 1408.09 (CP–Ca-US), indicating that the –COO– groups in Asp and Glu of the peptides might play a crucial role in calcium chelation.[20] The wavenumber of the amide II band at 1547.55 cm^{-1} (CP) shifted to 1555.81 cm^{-1} and 1555.26 cm^{-1} after the chelation, which also indicated the binding of the –COO– with Ca^{2+}.[10] No significant difference was observed in the FT-IR spectra between CP–Ca-HT and CP–Ca-US. These results provided evidence that Ca^{2+}

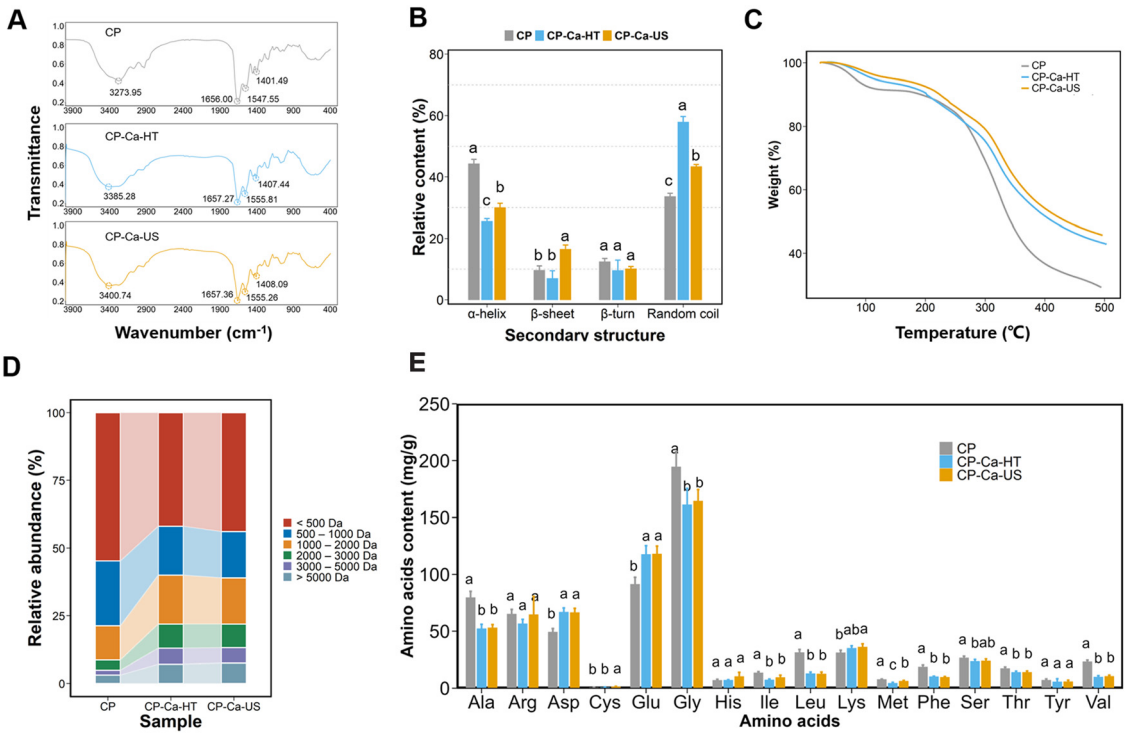

Fig. 2 Structural characterization properties. (A) FTIR spectra, (B) secondary structure, (C) thermogravimetric analysis, (D) molecular mass distribution, (E) amino acid content. CP: collagen peptides; CP–Ca-US: collagen peptide–calcium chelate prepared by the ultrasound method; CP–Ca-HT: collagen peptide–calcium chelate prepared by the hydrothermal method. Duncan's test was used to evaluate the significant differences between different groups. The different letters mean a significant difference between the two groups.

was chelated by CP to form CP–Ca-US, and the calcium-binding sites were the carboxyl oxygen and amino nitrogen atoms of Glu and Asp. These results were consistent with previous studies, such as white carp skin collagen peptides and whey peptides.[12,29]

3.2.2. Circular dichroism spectroscopy analysis. Fig. 2B shows the percentage composition of secondary structure deduced from the CD spectra. It is generally applied to investigate the structure change of proteins/peptides. The results indicated that the secondary structure was composed of α-helix, β-sheet, β-turn, and random coil. After calcium chelation, the α-helix structure for CP–Ca-HT and CP–Ca-US significantly decreased accompanied by a significant increase in the content of random coil structure. The result appeared that calcium-induced the structural change of CP from α-helix to the random coil. CP–Ca-HT and CP–Ca-US both showed structural transformation. This was consistent with previous studies that indicated that Ca^{2+} favored the decrease of α-helix structure of protein.[22,30] The secondary structures of CP–Ca-HT and CP–Ca-US showed similar results. These results indicated that chelated calcium ions could alter the spatial structure of peptides.

3.2.3. Thermal gravimetric analysis. The thermal stability of CP, CP–Ca-HT, and CP–Ca-US was evaluated by thermogravimetric analysis. As shown in Fig. 2C, during 25–200 °C, the weight of all samples showed a slight decrease due to the evaporation of moisture. During 200–400 °C, the weight of CP declined rapidly. Compared with CP, the weight of CP–Ca-HT and CP–Ca-US indicated a relatively slow decline at 200–400 °C. No significant difference was observed in the thermogravimetric curve between CP–Ca-HT and CP–Ca-US. The result indicated that CP–Ca-US exhibited high stability in the thermal environment. Because of the coordinate bonds between peptides and calcium ions, the thermal degradation of CP–Ca-US needed more energy to break chemical bonds.

3.2.4. Molecular mass distribution analysis. The molecular mass distribution of CP, CP–Ca-HT, and CP–Ca-US is shown in Fig. 2D. After the chelation reaction, the molecular mass distribution presented a significant change between CP and CP–Ca-US. The proportions of <500 Da, and 500–1000 Da in CP–Ca-US decreased significantly ($P < 0.05$), relative to those of CP. In contrast, the proportions of 1000–2000 Da, 2000–3000 Da, 3000–5000 Da, and >5000 Da increased. CP–Ca-HT and CP–Ca-US showed similar results without significant differences. The major reason may be the formation of supramolecular structures through coordination bonds and ionic bonds in CP–Ca-US, which caused the molecular mass to increase.

3.2.5. Amino acid component. The amino acid compositions of CP and CP–Ca-US are shown in Fig. 2E. Different types of amino acids contribute to the calcium-binding ability of peptides with different efficiencies.[31] In the chelate, the contents of Asp and Glu were significantly increased compared with those in CP ($P < 0.05$). Previous studies indicated that acidic amino acids were crucial to chelate metal ions due to

more active side chain groups, such as hydroxyl groups.[22,32,33] Qu *et al.*[31] also found increased content of Asp and Glu significantly, and Lys in peptide–iron chelate relative to before chelation. In this study, similar results were obtained that the content of Asp and Glu in CP–Ca-US had increased, but the difference of Lys did not reach a statistically significant level. This result was consistent with that from FT-IR analysis that the carboxyl oxygen and amino nitrogen atoms of Glu and Asp were the calcium-binding sites. The contents of Ala, Gly, Ile, Leu, Met, Phe, Thr, and Val in CP–Ca-US decreased signally ($P < 0.05$) indicating that non-polar amino acids and uncharged polar amino acids were not involved in the chelation reaction. Meanwhile, no significant difference was observed in the amino acid composition between CP–Ca-US and CP–Ca-HT.

3.2.6. Scanning electron microscopy analysis. SEM images were used to examine the microstructure of CP–Ca-HT and CP–Ca-US. The SEM is extensively used for microscale material and structure characterization. As shown in Fig. 3(A2, B2 and C2), collagen peptides presented a small partial structure with a smooth surface. After binding with calcium, CP–Ca-HT and CP–Ca-US exhibited clusters and large-sized particles. These observations agreed with a previous study, indicating that after binding peptide hydrophilic groups, the metal ions can promote aggregation, leading to the formation of compact particles.[34] EDS was carried out to determine the elemental compositions of CP and CP–Ca-US in detail, as shown in Fig. 3(A1, B1 and C1). There was a clear calcium peak in CP–Ca-US, which indicated that calcium ions had interacted with CP. As shown in Fig. 3(A3, B3 and C3), the elemental mapping image of CP indicated a weak signal of calcium, and the intensity of calcium signal was strong in CP–Ca-US. The element mapping image and EDS results confirmed the successful preparation of the peptide–calcium chelate. Meanwhile, no significant difference was observed in the SEM image, EDS, and elemental mapping image between CP–Ca-HT and CP–Ca-US. These results demonstrated that the chelation reaction could alter the microstructure of peptides, which was in line with the results of FT-IR and molecular mass distribution analysis.

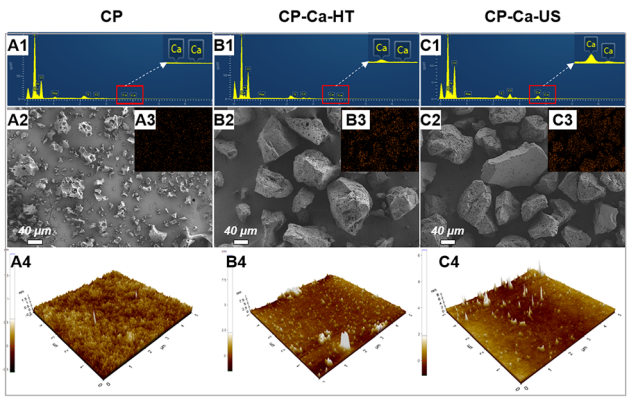

Fig. 3 Microstructure of CP–Ca-US. (A1–C1) Energy dispersive spectroscopy, (A2–C2) scanning electron microscope image, (A3–C3) element mapping image of calcium, (A4–C4) atomic force microscopy image. CP: collagen peptides; CP–Ca-US: collagen peptide–calcium chelate prepared by the ultrasound method; CP–Ca-HT: collagen peptide–calcium chelate prepared by hydrothermal method.

3.2.7. Atomic force microscopy analysis. The three-dimensional images of CP and CP–Ca-US are shown in Fig. 3(A4, B4 and C4). The AFM image of CP–Ca-US showed aggregates with larger particles. It may be due to the combination of calcium ions with the peptides, resulting in structural change and formation of larger particles, which were consistent with a previous study.[31] Compared with CPs–Ca-HT, the total number of particles of CPs–Ca-US increased, and the particle size decreased. The possible reason may be that ultrasound treatment could decrease the aggregation of peptides to form a small and uniform structure.[16]

3.2.8. Stability analysis. The stability of CP–Ca-US at different temperatures is shown in Fig. 4A. As the temperature increased from 50 °C to 80 °C, there was no significant effect of temperature on the calcium retention rate. The calcium retention rates of CP–Ca-US and CP–Ca-US presented the same results under different treatments. This result was in line with a previous study that peptide–calcium chelates exhibited good thermal stability.[11] CP–Ca-US could maintain high thermal stability (retention rate > 95%) in a wide temperature range (50–80 °C).

Dietary supplements are absorbed by the intestinal tract through gastrointestinal digestion, and biological activity may suffer undesirable effects due to unfavorable factors (H^+ and protease). Therefore, it is crucial to evaluate the digestive stability of CP–Ca-US in gastrointestinal digestion. To simulate the pH environment of the gastrointestinal tract, CP–Ca-US was dissolved in gastric pH (2.0) and intestinal pH (7.5) solutions without protease. As shown in Fig. 4B, the calcium retention rate of CP–Ca-US decreased significantly under gastric pH and gastric juice conditions ($P < 0.05$). It was speculated that high H^+ concentration under gastric conditions could compete with calcium ions to bind with NH^{3+} and $COOH^-$, which induced the Ca^{2+} release of CP–Ca-US. This result was consistent with the lower CCA under acidic conditions (pH = 5 and 6). Under intestinal pH conditions, the calcium retention rate of CP–Ca-US increased significantly compared with that of the control. This may be because the alkaline environment did not destroy the stable structure of the chelate and was beneficial for the chelation reaction. Under the gastric juice and intestinal juice, the calcium retention rate of CP–Ca-US decreased significantly ($P < 0.05$), compared with gastric pH and intestinal pH, respectively. It was speculated that peptides might be hydrolyzed by pepsin (gastric juice) and trypsin (intestinal juice) to form smaller peptides or amino acids, accompanied by the dissociation of the peptide–calcium chelate. A similar result was reported in a previous study that the re-chelation between peptides and Ca^{2+} was found to occur in a weak alkaline environment.[20] Wu *et al.*[11] indicated that the chelate stability was hardly affected by pepsin, and was sensitive to the change of pH value, which was consistent with the presented results. The calcium retention rate of CP–Ca-HT showed the same variation pattern as that of CP–Ca-US. It is worth noting that the calcium retention rates of CP–Ca-US increased under gastric juice and intestinal pH relative to that of CP–Ca-HT ($P < 0.05$).

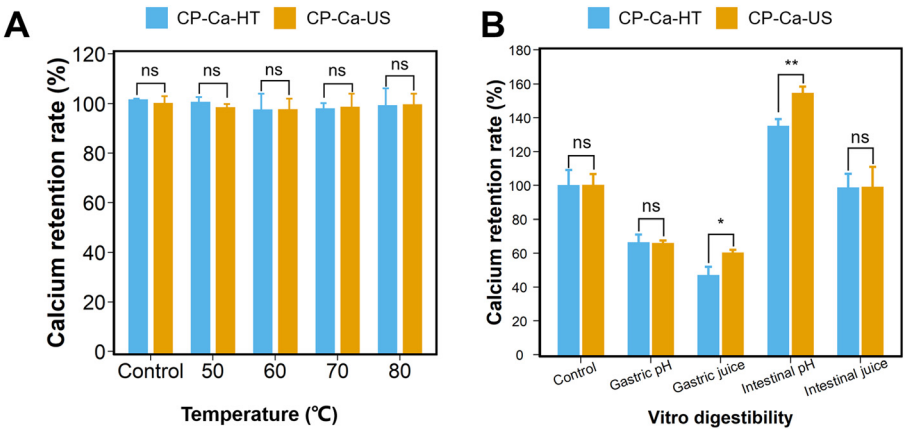

Fig. 4 Stability of CP–Ca-US. (A) Stability of chelate at various incubation temperature, (B) stability of the chelate at various digestive processes. CP: collagen peptides; CP–Ca-US: collagen peptide–calcium chelate prepared by ultrasound method; CP–Ca-HT: collagen peptide–calcium chelate prepared by the hydrothermal method. The statistical method is one-way ANOVA. The symbols indicate statistical significance: ns ($P > 0.05$), * ($P \leq 0.05$), ** ($P \leq 0.01$).

The possible reason may be the formation of more stable coordination bonds by the ultrasound method, caused by mechanical agitation and mixing, and the rise in local temperatures and pressures because of cavitation.[24] In the ultrasound process, not only thermal and mechanical effects but also cavitation effects have a significant effect on the chemical reaction. The cavitation effect can change the chemical processes in the system and enhance the rate of the reaction process or initiate new reaction mechanisms by forming various types of free radicals.[35] Due to the high stability of CP–Ca-US, it was selected to carry out follow-up cell experiments. Previous studies reported that the peptide–calcium chelate could promote calcium absorption across a Caco-2 cell monolayer.[10,11] Asai *et al.*[36] demonstrated that food-derived collagen peptides can be found in human blood. These pieces of evidence indicated that the peptide–calcium chelate could be absorbed through the gut. To further study the bioactivity of CP–Ca-US on bone building, the effect of CP–Ca-US on cell proliferation, cell cycle, and mineral deposition on MC3T3-E1 cells were investigated.

3.3. Effects of CP–Ca-US on MC3T3-E1 cells

3.3.1. Cell proliferation assay. The proliferation of CP–Ca-US for MC3T3-E1 cells was evaluated by the MTT assay. As shown in Fig. 5A, compared with the normal group, the proliferative bioactivity of CP–Ca-HT and CP–Ca-US significantly increased to 115–153%. With the increase of CP–Ca-US concentration, the proliferative rate gradually increased. When the concentration of CP–Ca-US reached 300 μg mL^{-1}, the proliferative rate was 153%. The osteoblast proliferation activity of CP–Ca-US displayed a dose dependent promotive effect. Compared with the normal group, $CaCl_2$ and CP + $CaCl_2$ did not show a significant difference, and their cell proliferation rates were 105% and 106%, respectively. Meanwhile, CP–Ca-US and CP–Ca-HT had higher cell proliferation rates than that of $CaCl_2$ and CP + $CaCl_2$. CP–Ca-US showed higher cell proliferation than CP–Ca-HT, but the difference did not reach a statistically significant level. Collagen peptides in the chelate could promote MC3T3-E1 cell proliferation by activating the PI3K/Akt pathway.[37] Chelates can significantly improve calcium absorption,[38] and a variety of proteins related to intracellular calcium ion signaling are involved in the regulation of cell proliferation.[39] Previous studies also found similar results that peptide–calcium chelates increase osteoblast proliferation, such as chelates from porcine bone and tilapia bone.[23,40]

3.3.2. Cell cycle alteration. As indicated in Fig. 5B, the proportion of the G0/G1 phase of MC3T3-E1 cells intervened by CP–Ca-US (>75 μg mL^{-1}) was lower ($P < 0.05$) than that of the normal cells. There was no significant difference between normal, $CaCl_2$, CP + $CaCl_2$, CP–Ca-HT (75), CP–Ca-US (75) groups. With the increase of concentration of CP–Ca-US, the percentage of the G2/M phase had increased ($P < 0.05$), and the percentage of the G0/G1 phase had increased ($P < 0.05$). This suggested that CP–Ca-US facilitated the transition of the cell cycle from the G0/G1 to G2/M phase. The observed cell cycle arrest at the G2/M phase suggested that CP–Ca-US may play a role in cell proliferation by promoting DNA synthesis. CP–Ca-US enhances the transfer and absorption of calcium, which could refer to the proliferation of the MC3T3-E1 cells. The calcium ion signals affect the changes in different cell cycle phases.[41]

3.3.3. Intracellular calcium ions. Calcium-sensing receptor (CaSR) is a class G-protein coupled receptor, which is widespread in prokaryotic and eukaryotic cells, regulating calcium and other metal ion homeostasis. To evaluate the mechanism of CP–Ca-US on calcium absorption, the effect of CaSR on intracellular calcium ions of the MC3T3-E1 cells was studied. In Fig. 5C, the Fluo-4/AM image in CP–Ca-US + R568 (CaSR agonist) presented a strong green fluorescence, followed by CP–Ca-US, CP–Ca-HT, and CP–Ca-US + Calhex231 (CaSR inhibitor). Then, the ImageJ software was applied to quantify the fluorescence intensity. As shown in Fig. 5D, the fluorescence intensity of calcium ions in the chelates (CP–Ca-HT and CP–Ca-US) increased significantly ($P < 0.05$) compared

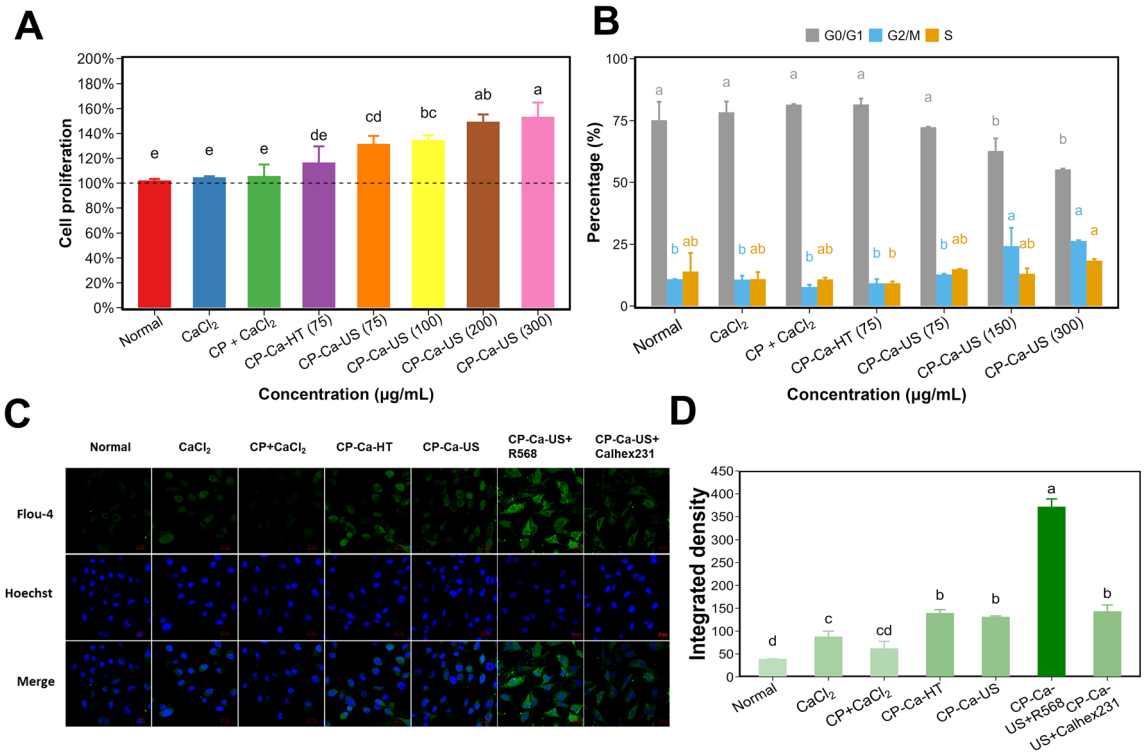

Fig. 5 (A) Effect of different concentrations of CP–Ca-US on the proliferation rate of MC3T3-E1 cells, (B) effect of different concentrations of CP–Ca-US on the cell cycle of MC3T3-E1 cells, (C) the intracellular calcium ions stained by Fluo-4/AM, (D) the relative green fluorescence intensity of Fluo-4/AM. CP: collagen peptides; CP–Ca-US: collagen peptide–calcium chelate prepared by the ultrasound method; CP–Ca-HT: collagen peptide–calcium chelate prepared by the hydrothermal method; R568: CaSR agonist; Calhex231: CaSR inhibitor. The numbers in parentheses represent concentrations (μg ml^{-1}). Duncan's test was used to evaluate the significant differences between different groups. The different letters mean the significant difference between the two groups.

with that in the normal, $CaCl_2$, and CP + $CaCl_2$ groups. It suggested that chelates could enhance calcium absorption. No significant difference was observed in the CP–Ca-HT and CP–Ca-US groups. CP–Ca-US could interact with the membrane and open calcium channels to influence calcium absorption. After the co-incubation of CP–Ca-US and R568, the fluorescence intensity of calcium increased significantly ($P < 0.05$) compared with that of the CP–Ca-US group. This indicated that CP–Ca-US induced the calcium ion influx may be related with CaSR. However, after the co-incubation of CP–Ca-US and Calhex231, the fluorescence intensity did not show a significant difference relative to that of CP–Ca-US. The main reason may be that calcium ions were absorbed not only through the CaSR pathway, but also through other pathways, such as TRPV5, TRPV6, and Cav1.3.[42] The specific calcium absorption mechanism remains to be further studied. These results indicated that CP–Ca-US enhanced the calcium absorption in the MC3T3-E1 cells by interacting with the CaSR.

3.3.4. Mineral deposition. As a marker of osteoblast differentiation and maturation, mineralization is also the main morphological features of osteoblasts performing osteogenic functions. Observing the mineralization level of osteoblasts is a commonly used technique for studying osteoblast differentiation. As shown in Fig. 6, compared with the normal group, the mineralization level in all treated groups had increased. The chelate (CP–Ca-US and CP–Ca-HT) showed an increased mineralization level compared with $CaCl_2$ and CP + $CaCl_2$. At the same concentration of 75 μg mL^{-1}, the mineralization level in CP–Ca-US was higher than that in CP–Ca-HT. This difference may be due to the higher stability of CP–Ca-US compared with CP–Ca-US. In the cytoplasm and on the cell surface, cellular proteases may destroy the structure of the chelate,[43] and CP–Ca-US might have high resistance against proteases. Meanwhile, with the increase of the CP–Ca-US concentration, the mineralization level gradually increased. This suggested that the differentiation activity of the CP–Ca-US for osteoblast cells exhibited a dose–response. However, the difference did not reach a statistically significant level among CP–Ca-US (75 μg mL^{-1}), CP–Ca-US (100 μg mL^{-1}), and CP–Ca-US (200 μg mL^{-1}). CP–Ca-US could improve calcium absorption by activating calcium/calmodulin mediated calcium/calmodulin-dependent protein kinase (CaMK2), and the increase in intracellular calcium concentration resulted in the activation of numerous targets including CaMK2, which plays a critical role in osteoblast differentiation.[44] This result was consistent with the above-mentioned results of calcium fluorescence imaging. On the other hand, CP–Ca-US could provide more calcium ions and a higher-density nucleation sites for mineral formation, which facilitated the mineralization process. The collagen peptides of the chelate could significantly increase ($P < 0.05$) the

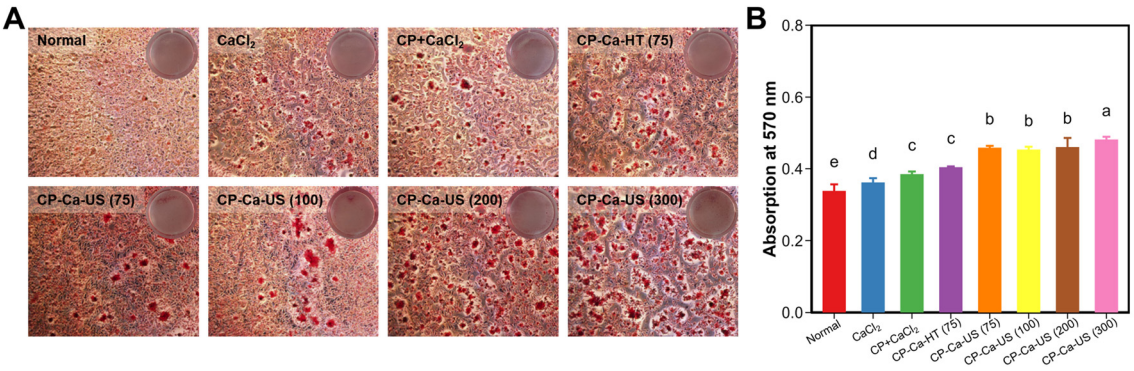

Fig. 6 (A) Effect of CP–Ca-US on mineralization of MC3T3-E1 cells. CP: collagen peptides, (B) quantitative analysis of binding of alizarin red dye to MC3T3-E1 cells. CP–Ca-HT: collagen peptide–calcium chelate prepared by the hydrothermal method. CP–Ca-US: collagen peptide–calcium chelate prepared by the ultrasound method. The numbers in parentheses represent concentrations (μg ml^{-1}). In CP + $CaCl_2$, peptides and calcium content were equal to those in CP–Ca-US (75 μg ml^{-1}). In $CaCl_2$, calcium content was equal to that in CP–Ca-US (75 μg ml^{-1}). Duncan's test was used to evaluate the significant differences between different groups. The different letters mean the significant difference between the two groups.

expression of Frizzled-5, β-catenin, Wnt5a, and GSK-3β.[45] The translocation of β-catenin from the cytoplasm to the nucleus functions combined with T cell factor enhancer lymphoid enhancer factor (TCF/LEF) to recruit coactivators, leading to the upregulation expression of target genes, such as Runt-related transcription factor 2 (Runx2) and osteoprotegerin (OPG). Runx2 and OPG are important transcription factors associated with the expression with osteoblast differentiation.[38,46] The proline in the collagen peptide sequence might also be contribute to the bioactivity of peptides.[47] Proline-rich peptides could promote osteogenic differentiation of MC3T3-E1 cells.[48] Wu *et al.*[23] also reported a similar result that porcine bone collagen peptides–calcium chelate enhanced the differentiation and mineralization on MC3T3-E1 cells. CaMKII is a serine–threonine kinase that is an important mediator of Ca^{2+} signaling in cells. Thus, we evaluated the interaction between CP–Ca-US and CaMKII by molecular docking. Molecular docking simulation is a frequently employed computer tool for predicting the binding affinity of protein–ligand complexes. Based on our previous study of the sequence of cattle bone collagen peptides,[34] the amino acid repeating sequence [Gly–X–Y]*n* (X and Y are mostly proline and hydroxyproline) of collagen, and Glu and Asp are important sites for calcium ions chelating with peptides,[49] the collagen peptides of SGE, TGE, AGE, ASGE, GEAGAQ, GPAGE, GPAGER, and GDTGAK were chosen to carry out molecular docking with CaMKII. Lu *et al.*[50] indicated that ligustilide (E-Lig) could bind with CaMKII as a potential drug target of suxiao jiuxin pill. Thus, E-Lig was chosen as a positive control to evaluate the interaction between collagen peptides and CaMKII. Generally, higher −CDOCKER energy and −CDOCKER interaction energy mean more stable and tighter binding between the receptor and the ligand. The conformation characterized by the highest −CDOCKER energy was selected as the most suitable conformation for each peptide. 10 collagen peptides that interacted with CaMKII are shown in Table S1 and Fig. S1–S4.† All the 10 collagen peptides could enter the receptor docking region, and their docking score was higher than E-Lig (positive control). The interaction between collagen peptide and CaMKII was mainly through non-covalent interactions, such as conventional hydrogen bond, and carbon hydrogen bond. These results indicated that CP–Ca-US might activate CaMKII by the collagen peptides to promote mineralization of osteoblasts.

4. Conclusions

In summary, a cattle bone-derived collagen peptide–calcium chelate prepared by the ultrasound method (CP–Ca-US) was successfully prepared and characterized, and the calcium-chelating ability reached 39.48 μg mg^{-1}. Various structural analyses confirmed that chelating sites of CP–Ca-US were carboxyl oxygen and amino nitrogen. CP–Ca-US showed a porous surface, large particles, high thermal stability, and digestive stability in intestinal digestion. CP–Ca-US showed more stability in gastric juice than the chelate prepared by the hydrothermal method. CP–Ca-US could significantly promote the proliferation and mineralization of MC3T3-E1 cells and promote calcium absorption by interacting with CaSR. CP–Ca-US is a promising calcium supplement to improve calcium bioactivity. Further studies will be focused on the peptide–calcium chelate absorption and transport mechanism.

Abbreviations

Ala	Alanine
Arg	Arginine
Asp	Aspartic acid
Cys	Cystine
Glu	Glutamic acid
Gly	Glycine
His	Histidine

Ile	Isoleucine
Leu	Leucine
Lys	Lysine
Met	Methionine
Phe	Phenylalanine
Ser	Serine
Thr	Threonine
Tyr	Tyrosine
Val	Valine

Conflicts of interest

All authors declare that they have no conflict of interest.

Acknowledgements

This work was supported by the Key Scientific and Technological Projects of Xinjiang Production and Construction Corps (2020AB012), the Technical Breakthrough Projects of Inner Mongolia Science and Technology Program (2022JBGS0007), and the Agricultural Science and Technology Innovation Program.

References

1 A. Erfanian, B. Rasti and Y. Manap, Comparing the calcium bioavailability from two types of nano-sized enriched milk using in-vivo assay, *Food Chem.*, 2017, **214**, 606–613.
2 M. Peacock, Calcium metabolism in health and disease, *Clin. J. Am. Soc. Nephrol.*, 2010, **5**, S23–S30.
3 J. M. Pettifor, Vitamin D &/or calcium deficiency rickets in infants & children: a global perspective, *Indian J. Med. Res.*, 2008, **127**, 245–249.
4 F. Bronner and D. Pansu, Nutritional aspects of calcium absorption, *J. Nutr.*, 1999, **129**, 9–12.
5 B. Tomadoni, C. Capello, G. A. Valencia and T. J. Gutiérrez, Self-assembled proteins for food applications: A review, *Trends Food Sci. Technol.*, 2020, **101**, 1–16.
6 Q. Xu, H. Hong, J. Wu and X. Yan, Bioavailability of bioactive peptides derived from food proteins across the intestinal epithelial membrane: A review, *Trends Food Sci. Technol.*, 2019, **86**, 399–411.
7 H. Ji, W. Zhao and Z. Yu, Interaction mechanism of three egg protein derived ACE inhibitory tri-peptides and DPPC membrane using FS, FTIR, and DSC studies, *Food Chem.: X*, 2022, **15**, 100366.
8 P. Cui, S. Lin, Z. Jin, B. Zhu, L. Song and N. Sun, In vitro digestion profile and calcium absorption studies of a sea cucumber ovum derived heptapeptide–calcium complex, *Food Funct.*, 2018, **9**, 4582–4592.
9 W. Liao, H. Chen, W. Jin, Z. Yang, Y. Cao and J. Miao, Three newly isolated calcium-chelating peptides from tilapia bone collagen hydrolysate enhance calcium absorption activity in intestinal Caco-2 cells, *J. Agric. Food Chem.*, 2020, **68**, 2091–2098.
10 A. Malison, P. Arpanutud and S. Keeratipibul, Chicken foot broth byproduct: A new source for highly effective peptide-calcium chelate, *Food Chem.*, 2021, **345**, 128713.
11 W. Wu, L. He, Y. Liang, L. Yue, W. Peng, G. Jin and M. Ma, Preparation process optimization of pig bone collagen peptide-calcium chelate using response surface methodology and its structural characterization and stability analysis, *Food Chem.*, 2019, **284**, 80–89.
12 L. Zhao, S. Huang, X. Cai, J. Hong and S. Wang, A specific peptide with calcium chelating capacity isolated from whey protein hydrolysate, *J. Funct. Foods*, 2014, **10**, 46–53.
13 Y. Song, Y. Fu, S. Huang, L. Liao, Q. Wu, Y. Wang, F. Ge and B. Fang, Identification and antioxidant activity of bovine bone collagen-derived novel peptides prepared by recombinant collagenase from Bacillus cereus, *Food Chem.*, 2021, **349**, 129143.
14 Y. Chen, Y. Guo, Y. Liu, C. Zhang, F. Huang and L. Chen, Identification of Di/Tripeptide(s) With Osteoblasts Proliferation Stimulation Abilities of Yak Bone Collagen by in silico Screening and Molecular Docking, *Front. Nutr.*, 2022, **9**, 874259.
15 K. L. Zapadka, F. J. Becher, A. L. Gomes dos Santos and S. E. Jackson, Factors affecting the physical stability (aggregation) of peptide therapeutics, *Interface Focus*, 2017, **7**, 20170030.
16 H. Li, Y. Hu, X. Zhao, W. Wan, X. Du, B. Kong and X. Xia, Effects of different ultrasound powers on the structure and stability of protein from sea cucumber gonad, *LWT – Food Sci. Technol.*, 2021, **137**, 110403.
17 L. Zhang, S. Zhao, S. Lai, F. Chen and H. Yang, Combined effects of ultrasound and calcium on the chelate-soluble pectin and quality of strawberries during storage, *Carbohydr. Polym.*, 2018, **200**, 427–435.
18 S. K. Ulug, F. Jahandideh and J. Wu, Novel technologies for the production of bioactive peptides, *Trends Food Sci. Technol.*, 2021, **108**, 27–39.
19 S. U. Kadam, B. K. Tiwari, C. Álvarez and C. P. O'Donnell, Ultrasound applications for the extraction, identification and delivery of food proteins and bioactive peptides, *Trends Food Sci. Technol.*, 2015, **46**, 60–67.
20 P. Cui, S. Lin, W. Han, P. Jiang, B. Zhu and N. Sun, Calcium delivery system assembled by a nanostructured peptide derived from the sea cucumber ovum, *J. Agric. Food Chem.*, 2019, **67**, 12283–12292.
21 H. Zhang, L. Zhao, Q. Shen, L. Qi, S. Jiang, Y. Guo, C. Zhang and A. Richel, Preparation of cattle bone collagen peptides-calcium chelate and its structural characterization and stability, *LWT – Food Sci. Technol.*, 2021, **144**, 111264.
22 N. Sun, Y. Wang, Z. Bao, P. Cui, S. Wang and S. Lin, Calcium binding to herring egg phosphopeptides: Binding characteristics, conformational structure and intermolecular forces, *Food Chem.*, 2020, **310**, 125867.
23 W. Wu, L. He, C. Li, S. Zhao, Y. Liang, F. Yang, M. Zhang, G. Jin and M. Ma, Phosphorylation of porcine bone col-

lagen peptide to improve its calcium chelating capacity and its effect on promoting the proliferation, differentiation and mineralization of osteoblastic MC3T3-E1 cells, *J. Funct. Foods*, 2020, **64**, 103701.

24 J. W. Chen and W. M. Kalback, Effect of ultrasound on chemical reaction rate, *Ind. Eng. Chem. Fundam.*, 1967, **6**, 175–178.

25 İ. Gülseren, D. Güzey, B. D. Bruce and J. Weiss, Structural and functional changes in ultrasonicated bovine serum albumin solutions, *Ultrason. Sonochem.*, 2007, **14**, 173–183.

26 L. Abadía-García, E. Castaño-Tostado, L. Ozimek, S. Romero-Gómez, C. Ozuna and S. L. Amaya-Llano, Impact of ultrasound pretreatment on whey protein hydrolysis by vegetable proteases, *Innovative Food Sci. Emerging Technol.*, 2016, **37**, 84–90.

27 P. Cui, N. Sun, P. Jiang, D. Wang and S. Lin, Optimised condition for preparing sea cucumber ovum hydrolysate–calcium complex and its structural analysis, *Int. J. Food Sci. Technol.*, 2017, **52**, 1914–1922.

28 W. Huang, Y. Lan, W. Liao, L. Lin, G. Liu, H. Xu, J. Xue, B. Guo, Y. Cao and J. Miao, Preparation, characterization and biological activities of egg white peptides-calcium chelate, *LWT – Food Sci. Technol.*, 2021, **149**, 112035.

29 X. Yang, X. Yu, A.-G. A. Yagoub, L. Chen, H. Wahia, R. Osae and C. Zhou, Structure and stability of low molecular weight collagen peptide (prepared from white carp skin)-calcium complex, *LWT – Food Sci. Technol.*, 2021, **136**, 110335.

30 J. Zhang, L. Liang, Z. Tian, L. Chen and M. Subirade, Preparation and in vitro evaluation of calcium-induced soy protein isolate nanoparticles and their formation mechanism study, *Food Chem.*, 2012, **133**, 390–399.

31 W. Qu, Y. Feng, T. Xiong, Y. Li, H. Wahia and H. Ma, Preparation of corn ACE inhibitory peptide-ferrous chelate by dual-frequency ultrasound and its structure and stability analyses, *Ultrason. Sonochem.*, 2022, **83**, 105937.

32 C. Torres-Fuentes, M. Alaiz and J. Vioque, Iron-chelating activity of chickpea protein hydrolysate peptides, *Food Chem.*, 2012, **134**, 1585–1588.

33 M. Chen, H. Ji, Z. Zhang, X. Zeng, W. Su and S. Liu, A novel calcium-chelating peptide purified from Auxis thazard protien hydrolysate and its binding properties with calcium, *J. Funct. Foods*, 2019, **60**, 103447.

34 H. Zhang, L. Zhao, Q. Shen, L. Qi and A. Richel, Preparation of cattle bone collagen peptides-calcium chelate and its structural characterization and stability, *LWT – Food Sci. Technol.*, 2021, **144**, 111264.

35 T. Kondo and E. Kano, Effect of free radicals induced by ultrasonic cavitation on cell killing, *Int. J. Radiat. Biol.*, 1988, **54**, 475–486.

36 T. Asai, A. Takahashi, K. Ito, T. Uetake, Y. Matsumura, K. Ikeda, N. Inagaki, M. Nakata, Y. Imanishi and K. Sato, Amount of collagen in the meat contained in Japanese daily dishes and the collagen peptide content in human blood after ingestion of cooked fish meat, *J. Agric. Food Chem.*, 2019, **67**, 2831–2838.

37 L. Zhu, Y. Xie, B. Wen, M. Ye, Y. Liu, K. M. S. U. Imam, H. Cai, C. Zhang, F. Wang and F. Xin, Porcine bone collagen peptides promote osteoblast proliferation and differentiation by activating the PI3K/Akt signaling pathway, *J. Funct. Foods*, 2020, **64**, 103697.

38 X. Wu, F. Wang, X. Cai and S. Wang, Characteristics and osteogenic mechanism of glycosylated peptides-calcium chelate, *Curr. Res. Food Sci.*, 2022, **5**, 1965–1975.

39 T. Sugimoto, M. Kanatani, J. Kano, H. Kaji, T. Tsukamoto, T. Yamaguchi, M. Fukase and K. Chihara, Effects of high calcium concentration on the functions and interactions of osteoblastic cells and monocytes and on the formation of osteoclast-like cells, *J. Bone Miner. Res.*, 1993, **8**, 1445–1452.

40 J. He, H. Guo, M. Zhang, M. Wang, L. Sun and Y. Zhuang, Purification and characterization of a novel calcium-binding heptapeptide from the hydrolysate of tilapia bone with its osteogenic activity, *Foods*, 2022, **11**, 468.

41 K. Machaca, Ca^{2+} signaling, genes and the cell cycle, *Cell Calcium*, 2011, **49**, 323–330.

42 K. Wongdee, K. Chanpaisaeng, J. Teerapornpuntakit and N. Charoenphandhu, in *Comprehensive Physiology*, ed. R. Terjung, Wiley, 1st edn, 2021, pp. 2047–2073.

43 A. Roessner, S. Krüger and A. Kido, Cellular proteases and invasion, *Verh. Deutsch. Ges. Path.*, 2000, **84**, 69–76.

44 G. Jung, Y. Park and J. Han, Effects of HA released calcium ion on osteoblast differentiation, *J. Mater. Sci.: Mater. Med.*, 2010, **21**, 1649–1654.

45 M. Ye, C. Zhang, L. Zhu, W. Jia and Q. Shen, Yak (Bos grunniens) bones collagen-derived peptides stimulate osteoblastic proliferation and differentiation via the activation of Wnt/β-catenin signaling pathway, *J. Sci. Food Agric.*, 2020, **100**, 2600–2609.

46 I. Hwang, E. Seo and H. Ha, Wnt/β-catenin signaling: A novel target for therapeutic intervention of fibrotic kidney disease, *Arch. Pharmacal Res.*, 2009, **32**, 1653–1662.

47 V. V. Andrushchenko, H. J. Vogel and E. J. Prenner, Solvent-dependent structure of two tryptophan-rich antimicrobial peptides and their analogs studied by FTIR and CD spectroscopy, *Biochim. Biophys. Acta, Biomembr.*, 2006, **1758**, 1596–1608.

48 M. Rubert, J. M. Ramis, J. Vondrasek, A. Gayà, S. P. Lyngstadaas and M. Monjo, Synthetic Peptides Analogue to Enamel Proteins Promote Osteogenic Differentiation of MC3T3-E1 and Mesenchymal Stem Cells, *J. Biomater. Tissue Eng.*, 2011, **1**, 198–209.

49 N. Sun, P. Cui, S. Lin, C. Yu, Y. Tang, Y. Wei, Y. Xiong and H. Wu, Characterization of sea cucumber (stichopus japonicus) ovum hydrolysates: calcium chelation, solubility and absorption into intestinal epithelial cells, *J. Sci. Food Agric.*, 2017, **97**, 4604–4611.

50 Y. Lu, J. Ji, S. Chu, F. Shen, W. Yang, W. Lei, M. Jiang and G. Bai, CaMKII, that binds with ligustilide, as a potential drug target of Suxiao jiuxin pill, a traditional Chinese medicine to dilate thoracic aorta, *Clin. Transl. Med.*, 2022, **12**, 907.